

# Structure-activity relationship of berberine and G4 DNA reveals aromaticity's effect on binding affinity

Sankrith Ramani<sup>1,2\*</sup>, Isha Tailor<sup>1,3\*</sup>, Smriti Kallahalla<sup>1,4\*\*</sup>, Stephanie Cheung<sup>1,5\*\*</sup>, Chloe Poon<sup>1,6\*\*</sup>, Vivek Parashar<sup>1,7</sup>, Harman Brah<sup>1</sup>

<sup>1</sup> Aspiring Scholars Directed Research Program, Fremont, California

<sup>2</sup> Langley High School, McLean, Virginia

<sup>3</sup> Dougherty Valley High School, San Ramon, California

<sup>4</sup> Henry M. Gunn High School, Palo Alto, California

<sup>5</sup> Abraham Lincoln High School, San Francisco, California

<sup>6</sup> Homestead High School, Cupertino, California

<sup>7</sup> Oswego East High School, Owego, Illinois

\*co-first authors, \*\*co-second authors

## SUMMARY

Secondary nucleic acid structures, such as the Guanine Quadruplex (G4), are known to contribute to gene regulation throughout the genome. In cancer cells, stabilizing such structures could prove to be integral to inhibiting cancer cell proliferation. Berberine is a natural quaternary alkaloid with a number of medicinal properties, including antimicrobial and anticancer effects. Previous studies have shown that berberine can stabilize the G4 through  $\pi$ - $\pi$  interactions, by increasing the release of free energy. In this study, we test the effectiveness of ligand aromaticity (cyclic, planar molecules) on the free energy of binding with the G4. Based on previous studies, we hypothesized that large aromatic rings incorporated in berberine molecules would act as highly stabilizing ligands that would generate the greatest binding affinity with the G4 through  $\pi$  interactions with guanine endplates and  $K^+$  ions. To explore the structure-activity relationship for berberine-based ligands, we developed an *in silico* library of 800+ ligands. Through molecular docking, we predicted the free energy release of each ligand's interaction with the G4 complex. From our research, we found that berberine analogs with aromatic R groups, which allow for high degrees of aromaticity and flexibility, have a significant positive impact on binding strength between berberine analogs and G4 complexes through  $\pi$ - $\pi$  interactions with endplates and grooves, indicating that these ligands can more effectively bind to and stabilize the G4's activity. The authors envision that this research may aid the development of drugs that target the G4 to inhibit cancer cell proliferation, ultimately furthering cancer therapeutics research.

## INTRODUCTION

In the 21st century, cancer is and will continue to be one of the leading causes of death in the United States (1). With the increase in risk factors in our environment — such as toxic chemicals, drug abuse, or chemical contaminants — as well as genetic and socioeconomic factors, susceptibility to

cancer will greatly increase (2). While recent developments in therapies, including immunotherapy and targeted therapies, have revolutionized anti-tumor care, increased focus on the genetic and epigenetic abnormalities in tumor cells have underscored the need for targeted molecular therapies (2).

The Guanine Quadruplex (G4) is a DNA/RNA quadruplex is a secondary nucleic acid structure that is present within telomeric DNA. It is formed in nucleic acids by sequences that have guanine and consist of guanine tetrads, a structure composed of four guanine bases in a square planar array. Past *in silico* analysis has shown that G4 structures regulate approximately 40% of genes within a 1 kb radius (3). Cation interactions,  $\pi$ - $\pi$  stacking, and halogenation lead to more thermodynamically favorable binding, which increases the free energy of binding and electrostatic potential between ligands and the G4, stabilizing the G4 and enabling it to regulate telomere elongation (4). Furthermore, because of their presence within most human oncogenic promoters and telomeres, G4 structures are currently being tested as a therapeutic target to down-regulate transcription or block telomere elongation in cancer cells (2).

The G4's main anti-tumor mechanism lies in its ability to regulate telomere elongation. Telomeres are regions of repetitive DNA sequence at the ends of chromosomes that protect the chromosomes. Every time a cell divides, telomeres become shorter; eventually, they become so short that the cell no longer divides successfully and dies. The enzyme telomerase is responsible for maintaining the length of telomeres via guanine-rich sequence addition (5). In normal somatic cells, telomerase activity is extremely limited. For every normal cell cycle, 50 nucleotides are lost, resulting in a gradual decrease of telomere length; when the telomere is critically short, it triggers senescence, blocking further cell division. However, in tumor cells, the system of telomere length maintenance is activated, thus encouraging uncontrolled cell division (6). Ligands that can bind to and stabilize the G4 can inhibit this length maintenance process, allowing for the inhibition of telomerase to arrest the uncontrollable cell cycle of tumor cells (Figure 1).

Berberine is an isoquinoline quaternary alkaloid with implications for the treatment of cancer because it induces apoptosis in cancer cell lines (7,8). It binds to G4-DNA by  $\pi$ - $\pi$  stacking interactions (9). Berberine binds to G4-DNA with



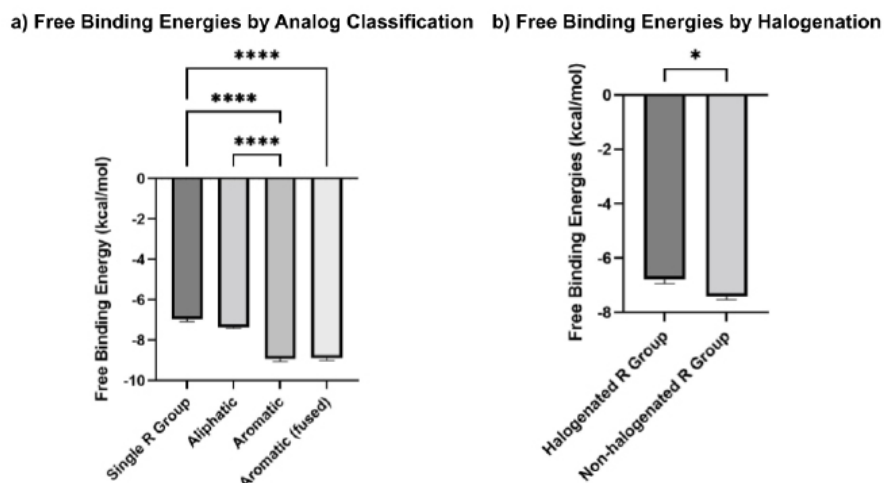


**Figure 2: Free energy release for berberine ligand interactions with G4.** 836 berberine analogs were grouped into four R-group classes: 51 single R groups, 264 aliphatic sidechains, 267 aromatic sidechains and 247 aromatic sidechains. Within single atom R groups, the analogs were further split into halogenated R groups and non-halogenated R groups. Binding energies obtained from molecular docking analysis were tabulated and graphed for each analog class. (A) Binding energies compared across analog classes. Free energy release was significantly greater for aromatic R groups than aliphatic R groups. A one-way ANOVA test was conducted, with the R-group classification as the independent variable, and the free binding energy as the dependent variable ( $F = 64.81$ ,  $p < 0.0001$ ). \*\*\*\* $p < 0.0001$ . (B) Binding energies compared between halogenated and non-halogenated single R groups. Free energy release was significantly greater for halogen R groups than other R groups. \* $p < 0.01$ . Error bars = standard error of the mean.

contacts between the G4 and berberine analogs showed that the number of electrostatic interactions did not correlate to any changes in the free energy of binding, ruling it out as a contributing factor to G4 stabilization.

### Higher binding affinities trade-off with practical drug delivery characteristics

While ligands with large aromatic rings and high degrees of flexibility were found to achieve the most thermodynamically favorable interactions with the G4, there are trade-offs with other molecular properties important for drugs. The highest binders from each analog class were assessed for their physicochemical and pharmacological properties, including solubility, molecular weight, octanol-water partition coefficient, bioavailability, and synthetic accessibility. The

ligands with large aromatic rings are much less soluble and thus have a lower bioavailability than ligands with single R groups or aliphatic sidechains (Table 2). While this could be offset with modern developments in water-insoluble drug delivery technology, decreasing the solubility of the ligand by adding large aromatic groups could lower the accessibility of the drug, from both a drug-delivery and drug-synthesis standpoint. One standout aromatic molecule in the series is D5, which has a high free binding energy of -10.1 kcal/mol, and a moderate bioavailability of 0.55.

### DISCUSSION

We performed molecular docking with berberine analogs and the G4 to assess the structure-activity relationship between the aromaticity of the berberine analog, the type of  $\pi$  interactions, and the free energy of binding. The most thermodynamically favorable binders had aromatic R groups, whether fused or attached to berberine and engaged in  $\pi$  interactions with either the  $K^+$  ions or the grooves of the G4 (Figure 2). Analysis of the molecular docking and molecular visualization revealed two main factors in the binding of berberine to G4: the location and structure of the binding area on the G4, as well as the physical structure of the berberine analog's R groups (Table 1).

While we observed most of the contact between the G4 and berberine analogs occurring with the G4 endplates near the  $K^+$  ions, interactions with the grooves of the G4 were also an important contributor to the free energy of binding. Berberine analogs with fused aromatic R groups had a small average distance from the G4 ranging from 2.6 Å to 5.2 Å and a large number of aromatic rings with delocalized  $\pi$  electron clouds; the proximity of the  $K^+$  ions to the berberine molecule likely allowed the  $K^+$  ions' positive charge to polarize the  $\pi$  electron clouds, leading to the high binding free energies of the thermodynamically favorable  $\pi$ -cation interactions. Berberine analogs with aromatic R groups that weren't

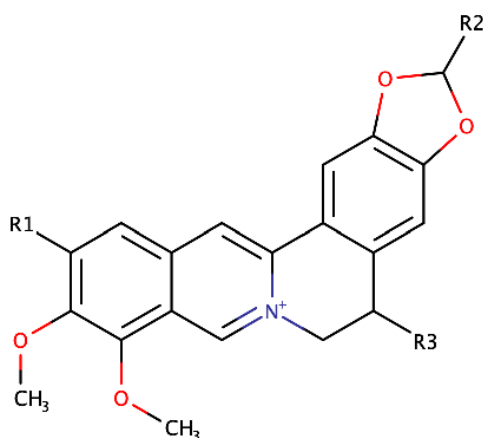


**Figure 3: Locations of documented R groups on berberine.** Our analogs had R groups attached to three particular locations on the berberine molecule; to maximize the stability of the molecule and its binding properties with the G4 molecule.

ID	R1	R2	R3	$\Delta G$	ES:	$\pi$	ID	R1	R3	$\Delta G$	ES:	$\pi$	$\bar{A}$
A1	F	F	F	-8.1	487	5.2	C1			-12.6	1751	n- $\pi$ with endplates and grooves	5.2
A2		Cl	Cl	-8.0	688	4.7	C2			-12.2	1179	n- $\pi$ with endplates and grooves	5.4
A3	I	I	I	-8.0	915	4.5	C3			-11.0	1287	n- $\pi$ with endplates	4.7
A4	OH		OH	-7.6	544	4.9	C4			-10.7	1436	n-cation with K+	3.1
A5	NH2	NH2	Cl	-7.2	563	5.9	D1			-14.7	671	n-cation with K+	2.6
B1				-10.0	1034	5.1	D2			-14.0	596	n-cation with K+	3.0
B2				-9.6	654	3.6	D3			-11.6	605	n- $\pi$ with endplates	3.0
B3				-9.4	954	5.3	D4			-11.1	825	N/A	5.0
B4				-9.3	899	5.2	D5			-10.1	866	N/A	5.2
B5				-9.2	1057	3.5							

**Table 1: Summary of berberine analogs with highest binding affinity to G4.** The top 5 binders from each analog class, as found by our molecular docking data, were selected from our 836-ligand library. Using molecular visualization, we tabulated the location of R groups (as highlighted in Figure 3), binding affinity energy values ( $\Delta G$  in kcal/mol). Furthermore, we analyzed how the ligands bound to the G4 by quantifying the number of electrostatic contacts (ES),  $\pi$ - $\pi$  interactions, and average distance of the ligand from the G4.  $\pi$ - $\pi$  interactions were only quantified for aromatic R groups, as other R groups cannot engage in  $\pi$ - $\pi$  stacking. Results indicate that while electrostatic interaction did not have an observationally significant effect on  $\Delta G$ ,  $\pi$  interactions with endplate grooves contributed to a higher binding activity with the G4.

fused, however, had larger average distances while still maintaining high binding free energies through  $\pi$  interactions with the grooves of the G4, especially in comparison to that

of unmodified berberine. Due to a combination of their large surface area, aromaticity, and flexibility owing to lack of fused aromatic R groups, these analogs were able to bind with both

ID	Solubility (mol/L)	Solubility Class	Weight (g/mol)	# HBond Acceptors	# HBond Donors	log P	Bioavailability	Synthetic Accessibility
A1	$6.93 \times 10^0$	Moderately soluble	390.33	7	0	3.13	0.55	4.19
A2	$3.02 \times 10^6$	Moderately soluble	405.25	4	0	2.63	0.55	3.99
A3	$7.97 \times 10^9$	Poorly soluble	714.05	4	0	3.74	0.55	4.20
A4	$1.64 \times 10^6$	Soluble	368.36	6	2	0.84	0.55	3.69
A5	$8.36 \times 10^3$	Moderately soluble	400.84	5	2	1.47	0.55	4.17
B1	$2.95 \times 10^0$	Moderately soluble	530.54	10	2	2.38	0.17	5.39
B2	$8.73 \times 10^{-2}$	Moderately soluble	447.37	11	2	3.84	0.55	4.26
B3	$3.65 \times 10^8$	Poorly soluble	544.77	4	0	1.66	0.55	4.64
B4	$9.50 \times 10^5$	Moderately soluble	437.43	9	0	1.17	0.55	4.47
B5	$1.04 \times 10^5$	Moderately soluble	418.80	7	0	13.24	0.55	3.99
C1	$5.41 \times 10^7$	Poorly soluble	595.57	13	0	3.57	0.17	4.67
C2	$2.42 \times 10^{17}$	Insoluble	1057.25	4	0	14.27	0.17	7.60
C3	$3.98 \times 10^{11}$	Insoluble	657.61	9	0	9.64	0.17	4.43
C4	$2.79 \times 10^{17}$	Insoluble	973.96	4	0	13.15	0.17	5.79
D1	$7.74 \times 10^{22}$	Insoluble	1197.79	2	0	17.86	0.17	5.39
D2	$1.48 \times 10^{16}$	Insoluble	876.96	4	0	15.93	0.17	5.27
D3	$1.09 \times 10^{10}$	Poorly soluble	558.62	4	0	7.91	0.17	4.54
D4	$3.27 \times 10^8$	Poorly soluble	672.49	11	0	4.96	0.17	5.34
D5	$8.34 \times 10^9$	Poorly soluble	485.53	4	1	6.12	0.55	3.56

**Table 2: Physicochemical and pharmacological properties of analogs with highest binding affinity to G4.** Each series in Table 1 was selected and the physicochemical and pharmacological properties of the ligands were evaluated. Log P refers to the octanol-water partition coefficient, which measures the relationship between lipophilicity and hydrophilicity of a substance. The data underscores that ligands with large aromatic rings are poorly soluble or insoluble, while ligands with single R groups or aliphatic chains tend to be moderately soluble.

the endplates of the G4 and fit into the grooves of the G4 complex, resulting in more energetically favorable binding (Table 1).

Our study suggests that for the berberine ligand to engage in  $\pi$  interactions with the G4 endplates,  $K^+$  cations, and grooves, aromatic R groups (fused or not fused) are preferable. We found that the aromaticity of R groups led to significant higher binding free energies compared to that of the unmodified berberine (Figure 2). This is likely due to a greater amount of delocalized  $\pi$  orbitals that can interact with the G4 (10,11). We also found, through molecular visualization, that mere size of the aromatic R groups didn't affect the free energy of binding; the free energy of binding was more dependent on the types of  $\pi$  interactions and the flexibility of the molecules (Table 1). The flexibility of the analogs was essential to forming thermodynamically favorable interactions with high binding free energies: aromatic R groups that were not fused had a high degree of flexibility due to the alkanes connecting the rings that allowed the molecules to bind to both the endplates, the  $K^+$  ions, and the grooves of the G4.

Further, we also found that halogenated functional groups had a slight impact on binding free energies: analogs from all four classes, especially single atom R groups, that contained halogens in their R groups had higher binding free energies. We speculate that halogenation resulted in an attraction between the halogen and the  $K^+$  cation in the G4 model (Figure 2) (4). In addition, we suspect a correlation between electronegativity and free energy of binding, since between the halogenated R groups, the ones with fluorine, a high-electronegativity atom, had the highest free energy of binding of the series (Table 1).

Finally, since berberine's effectiveness in cancer therapy

lies first and foremost in its abilities as a drug, extended research should continue to explore what factors lend to these ideal conditions for drug delivery. Future studies testing berberine analogs to maximize free binding energy should take into account the practical limitations of using such large ligands as therapeutics.

G4 stabilization is a growing and promising field of research within cancer research and can even extend beyond cancer to other biological applications involving regulating DNA transcription (2). Trends observed in our library provide future considerations for G4 stabilization using berberine, underscoring the importance of G4 endplate binding brought about by engineered molecules with a large surface area, high degree of aromaticity, and high degree of flexibility. Future studies should concentrate on isolating variables such as number of atoms, aromatic carbons, and rotatable bonds to provide a more granular analysis of the structural factors that allow for strong G4 binders. Focused *in silico* studies testing specific R groups, such as iron complexes, could provide further insight into the precise binding mechanisms of the G4 to various types of R groups. Further testing involving assays that can probe the stabilizing effects of these binders *in vivo* and *in vitro* can test the efficacy of these ligands for pharmaceutical use. We hope this research may aid the development of ligands to stabilize the G4 through the trends identified in berberine ligand structure-activity relationships.

## MATERIALS AND METHODS

### Ligand Design and Pre-Optimization

We developed a library of 800+ ligands. The visualization and development of the ligands were done initially on MarvinSketch (by ChemAxon) wherein we attached varied

substrates at different R-group locations to the 2-D berberine molecule (16). Avogadro, a cross-platform molecular editor, was used to optimize molecules by molecular mechanics using the Merck Molecular Force Field (MMFF94) to 10,000 steps, prior to density functional theory (DFT) geometry optimization, by industry standards (17).

### DFT Optimization

DFT is a quantum mechanical modeling procedure that employs the use of electronic density to calculate the electronic structure and ground state energies of atoms and molecules (18). In this case, DFT calculated the most quantum-mechanically optimal configurations for the berberine analogs before the molecular docking procedures. In combination with Avogadro, Orca (an *ab initio* quantum mechanical molecular modeling software) was used to generate input files to conduct DFT calculations for berberine analogs (19). The hybrid functional B3LYP was chosen to conduct calculations, as it is the most widely accepted and mathematically reliable functional (20). To simulate aqueous conditions, a conductor-like polarizable membrane (CPCM) water model was used. The def2-SVP basis set was used for calculations, as the analog library contained compounds composed of light main-group elements.

### Molecular Docking

Prior to docking, AutoDock Tools (a graphical user interface that allows for preparation and generation of coordinate files) was used to prepare ligands for docking. AutoDock Tools identified receptors as macromolecules, adding Gasteiger charges to the ligand and merging non-polar hydrogens. Each ligand was imported into AutoDock tools, upon which the above processes were applied to the molecule. AutoDock Vina is a molecular docking software allowing for the modeling of ligand-protein interaction thermodynamics. Vina allowed us to simulate docking the berberine analogs to the G4. They were imported into AutoDock Vina, where they were docked to a G4 (PDB ID 1KF1), using an exhaustiveness of 8 (21).

### UCSF Chimera/ChimeraX

Chimera and ChimeraX were used for the final visualization and analysis of the binding free energies, following the computational binding of the affected berberine molecules to the G4 (22,23).

### SwissADME

SwissADME was used to assess the physiochemical and pharmacological properties of selected ligands (molecular weight, hydrogen bond acceptors and donors, octanol-water partition coefficient, solubility, bioavailability score, synthetic accessibility) (24). The logarithm of the partition coefficient (P) was determined using a topological method from Lipinski *et al.* 2001 (25). Solubility was determined by implementing a topological method from Delaney 2004 (26), and solubility class was determined by the following criteria on the Logarithm of Solubility (Log S) scale: Insoluble (Log S < -9), Poorly soluble (Log S < -6), Moderately soluble (Log S < -4), and Soluble (Log S < -2). Bioavailability was determined with a probability <10% derived from a Fisher-Snedecor distribution (F), as implemented in Martin 2005 (27). Synthetic accessibility was scored from 1 (very easy) to 10 (very difficult), based on 1024 fragmental contributions

modulated by size and complexity and trained on 12,782,590 molecules ( $r^2 = 0.94$ ).

**Received:** February 11, 2022

**Accepted:** September 5, 2022

**Published:** March 3, 2023

### REFERENCES

1. Nagai, Hiroki, and Young Hak Kim. "Cancer Prevention from the Perspective of Global Cancer Burden Patterns." *Journal of Thoracic Disease*, vol. 9, no. 3, 15 Mar. 2017, pp. 448–451., doi:10.21037/jtd.2017.02.75.
2. Kosiol, Nils, *et al.* "G-Quadruplexes: A Promising Target for Cancer Therapy." *Molecular Cancer*, vol. 20, no. 1, 2021, doi:10.1186/s12943-021-01328-4.
3. Fujiwara, Nana, *et al.* "TMPYP4, a Stabilizer of Nucleic Acid Secondary Structure, Is a Novel Acetylcholinesterase Inhibitor." *PLOS ONE*, vol. 10, no. 9, 2015, doi:10.1371/journal.pone.0139167.
4. Moye, Aaron L., *et al.* "Telomeric G-Quadruplexes Are a Substrate and Site of Localization for Human Telomerase." *Nature Communications*, vol. 6, no. 1, 2015, doi:10.1038/ncomms8643.
5. Jafri, Mohammad A., *et al.* "Roles of Telomeres and Telomerase in Cancer, and Advances in Telomerase-Targeted Therapies." *Genome Medicine*, vol. 8, no. 1, 2016, doi:10.1186/s13073-016-0324-x.
6. Grycová, Lenka, *et al.* "Quaternary Protoberberine Alkaloids." *Phytochemistry*, vol. 68, no. 2, 15 Nov. 2007, pp. 150–175., doi:10.1016/j.phytochem.2006.10.004.
7. Wang, Ye, *et al.* "The Anti-Cancer Mechanisms of Berberine: A Review." *Cancer Management and Research*, Volume 12, 30 Jan. 2020, pp. 695–702., doi:10.2147/cmar.s242329.
8. Cao, Qian, *et al.* "G-Quadruplex DNA Targeted Metal Complexes Acting as Potential Anticancer Drugs." *Inorganic Chemistry Frontiers*, vol. 4, no. 1, 30 Sept. 2017, pp. 10–32., doi:10.1039/c6qi00300a.
9. Arora, Amit, *et al.* "Binding of Berberine to Human Telomeric Quadruplex - Spectroscopic, Calorimetric and Molecular Modeling Studies." *FEBS Journal*, vol. 275, no. 15, 2008, pp. 3971–3983., doi:10.1111/j.1742-4658.2008.06541.x.
10. Papi, Francesco, *et al.* "Pyridine Derivative of the Natural Alkaloid Berberine as Human Telomeric G4-DNA Binder: A Solution and Solid-State Study." *ACS Medicinal Chemistry Letters*, vol. 11, no. 5, 2020, pp. 645–650., doi:10.1021/acsmchemlett.9b00516.
11. Ruehl, Carmen L., *et al.* "An Octahedral Cobalt(III) Complex with Axial NH<sub>3</sub> Ligands That Templates and Selectively Stabilises G-Quadruplex DNA." *Chemistry – A European Journal*, vol. 25, no. 41, 2019, pp. 9691–9700., doi:10.1002/chem.201901569.
12. Chen, Shuo-Bin, *et al.* "The Role of Positive Charges on G-Quadruplex Binding Small Molecules: Learning from Bisaryldiketene Derivatives." *Biochimica Et Biophysica Acta (BBA) - General Subjects*, vol. 1830, no. 11, 20 July 2013, pp. 5006–5013., doi:10.1016/j.bbagen.2013.07.012.
13. Spiegel, Jochen, *et al.* "The Structure and Function of DNA G-Quadruplexes." *Trends in Chemistry*, vol. 2, no. 2, 31 July 2020, pp. 123–136., doi:10.1016/j.trechm.2019.07.002.

14. Meyer, Michael, *et al.* "Are Guanine Tetrads Stabilized by Bifurcated Hydrogen Bonds?" *The Journal of Physical Chemistry A*, vol. 105, no. 35, 2001, pp. 8223–8225., doi:10.1021/jp011179i.
15. González-Rodríguez, David, *et al.* "G-Quadruplex Self-Assembly Regulated by Coulombic Interactions." *Nature Chemistry*, vol. 1, no. 2, 19 Apr. 2009, pp. 151–155., doi:10.1038/nchem.177.
16. Ertl, Peter. "Molecular Structure Input on the Web." *Journal of Cheminformatics*, vol. 2, no. 1, 2 Feb. 2010, doi:10.1186/1758-2946-2-1.
17. Hanwell, Marcus D, *et al.* "Avogadro: An Advanced Semantic Chemical Editor, Visualization, and Analysis Platform." *Journal of Cheminformatics*, vol. 4, no. 1, 2012, doi:10.1186/1758-2946-4-17.
18. Orio, Maylis, *et al.* "Density Functional Theory." *Photosynthesis Research*, vol. 102, no. 2-3, 2009, pp. 443–453., doi:10.1007/s11120-009-9404-8.
19. Neese, Frank, *et al.* "The Orca Quantum Chemistry Program Package." *The Journal of Chemical Physics*, vol. 152, no. 22, 2020, p. 224108., doi:10.1063/5.0004608.
20. Becke, Axel D. "Density-Functional Thermochemistry. III. the Role of Exact Exchange." *The Journal of Chemical Physics*, vol. 98, no. 7, 1993, pp. 5648–5652., doi:10.1063/1.464913.
21. Trott, Oleg, and Arthur J. Olson. "Autodock Vina: Improving the Speed and Accuracy of Docking with a New Scoring Function, Efficient Optimization, and Multithreading." *Journal of Computational Chemistry*, vol. 31, 2009, doi:10.1002/jcc.21334.
22. Huang, Conrad C., *et al.* "Enhancing UCSF Chimera through Web Services." *Nucleic Acids Research*, vol. 42, no. W1, 2014, doi:10.1093/nar/gku377.
23. Goddard, Thomas D., *et al.* "UCSF Chimerax: Meeting Modern Challenges in Visualization and Analysis." *Protein Science*, vol. 27, no. 1, 2017, pp. 14–25., doi:10.1002/pro.3235.
24. Daina, Antoine, *et al.* "SwissADME: A Free Web Tool to Evaluate Pharmacokinetics, Drug-Likeness and Medicinal Chemistry Friendliness of Small Molecules." *Scientific Reports*, vol. 7, no. 1, 2017, doi:10.1038/srep42717.
25. Lipinski, Christopher A., *et al.* "Experimental and Computational Approaches to Estimate Solubility and Permeability in Drug Discovery and Development Settings." *Advanced Drug Delivery Reviews*, vol. 64, 2001, pp. 4–17., doi:10.1016/j.addr.2012.09.019.
26. Delaney, John S. "ESOL: Estimating Aqueous Solubility Directly from Molecular Structure." *Journal of Chemical Information and Computer Sciences*, vol. 44, no. 3, 2004, pp. 1000–1005., doi:10.1021/ci034243x.
27. Martin, Yvonne C. "A Bioavailability Score." *Journal of Medicinal Chemistry*, vol. 48, no. 9, 2005, pp. 3164–3170., doi:10.1021/jm0492002.

**Copyright:** © 2023 Ramani, Tailor, Kallahalla, Cheung, Poon, Parashar, and Brah. All JEI articles are distributed under the attribution non-commercial, no derivative license (<http://creativecommons.org/licenses/by-nc-nd/3.0/>). This means that anyone is free to share, copy and distribute an unaltered article for non-commercial purposes provided the original author and source is credited.